Estimating Parameters of Received UWB Monocycles

Chee-Cheon Chui and Robert A. Scholtz
UltRaLab, Communication Sciences Institute, USC
Los Angeles, CA 90089

Abstract: **This work assumes that local oscillators in individual transceivers are not identical. A difference in the drift of oscillator gives rise to a difference in pulse repetition rate between transmitter and receiver. This drift will be estimated in the paper. The performance of a proposed Automated Gain Control (AGC) circuit to stabilize the gain of a time tracking loop is also investigated. Thus this work is on estimating the received signal amplitude, the initial offset and frame frequency differences between a pair of UWB impulse transceiver and the results will be useful for applications such as time transfer and synchronization.**

I. Introduction

Many recent works, e.g. [3], have analyzed the acquisition and tracking of UWB impulse radio. Most of these works do not consider the fact that local oscillators are not identical in individual transceivers. In the simplest scenario, a difference in first order drift of oscillator gives rise to a difference in pulse repetition rate between transmitter and receiver. This difference in oscillator drift is usually ignored in narrowband carrier based systems. However, in UWB impulse radio, the effective pulse width of the monocycles is very small, typically in the order of sub-nanoseconds. To ignore this difference in oscillator drift between UWB transmitter and receiver may lead to performance degradation.

Using tracking loop to mitigate difference in frame repetition frequency and delay in received UWB signals has been addressed in [5]. This work concentrates on estimating the initial offset and frame frequency differences by measuring the Time-of-Arrival (ToA) of the transmitted monocycle at the receiver in the presence of additive noise. The major sources of impairments to the ToA measurement are additive noise, oscillator phase noise, multipath self-interference and NLOS measurements that give a positive bias to the ToA readings [7]. For UWB impulses fully utilizing the FCC indoor spectral mask, which is assumed herewith, the bias on the ToA measurements attributed to multipath self interference is assumed negligible [6]. The effect of both transmitter and receiver oscillators' phase noise, and Non-Line-of-Sight (NLOS) measurement error are treated in [8] and will not be repeated here. This paper expands on [5] and analyzes in detail the effects of a feedforward Automated Gain Control (AGC) loop to stabilize the amplitude of the processed UWB monocycle.

Reference [1] provides an excellent summary of the working of AGC for narrowband communications signal riding on a carrier. An impulse UWB system possibly excludes the use of bandpass limiter and a narrow pulse width instead of a constant signal envelope presents new challenges to an effective AGC for UWB impulse radio. In this paper, a correlative feedforward AGC designed primarily for UWB impulse radio is investigated. In the absence of perfect knowledge about the received signal amplitude, the importance of the AGC in adjusting the gain of the TLL is illustrated.

This work assumes that there is no interframe interference, which is to a certain extent guaranteed by a low duty cycle system for applications such as ranging, time transfer and geolocation. It is also assumed that there is no relative movement between transceivers during a measurement cycle.

II. System Model

A local oscillator with phase $\Phi^{(m)}(t)$ generates an imperfect timing function defined by

$$T^{(m)}(t)=\Phi^{(m)}(t)/\omega_o \tag{1a}$$

where ω_o is the oscillator nominal frequency. The superscript in parenthesis $(\circ)^{(m)}$ is used to denote transceiver (m). The random phase jitter of the oscillator is assumed negligible compared to channel noise and ignored in following analysis. Readers are referred to [1] and [13] for more details on timing function generated by oscillator.

It is assumed that the positive-going zero crossings of an oscillator with timing function given by (1a) are used to trigger the transmission of UWB impulses, i.e., pulses are transmitted at oscillator time $T(t_k^{(m)})=kT_f$ where $t_k^{(m)}$ is:

$$t_k^{(m)}=a_1^{(m)}kT_f+d^{(m)} \tag{1b}$$

The deterministic parameter $a_1^{(m)}=1\pm\eta$ for $\eta\leq 10^{-6}$, modeled the first order drift of the oscillator and $d^{(m)}$ is the oscillator initial offset. The receiver, denoted as (s), generates a reference signal, the purpose of which is to correlate with the received signal to derive the ToA of the received monocycles. These reference monocycles are generated at $T^{(s)}(t_k^{(s)})=kT_f$ where, defined similarly as in (1b):

$$t_k^{(s)}=a_1^{(s)}kT_f+d^{(s)}\,. \tag{1c}$$

Therefore the received and reference UWB signals at receiver (s) are written as:

$$y^{(s)}(t)=A_w\sum_{k'}w\left(t-a_1^{(m)}k'T_f-d^{(m)}-\tau_{m,s}\right)+n(t) \tag{2a}$$

$$f^{(s)}(t)=A_r\sum_k r\left(t-a_1^{(s)}kT_f-d^{(s)}\right) \tag{2b}$$

This work is supported in part by a MURI Project under Contract DAAD 19-01-1-0477 from the US Army Research Office. Chee-Cheon Chui's postgraduate study in USC is supported by DSO National Laboratories, Singapore.

where $k, k' \in \{0,1,2,3,4,...\}$, $n(t)$ is the additive noise in the channel with one-sided power density N_o, $T_f = 1/\omega_o$ and there is one monocycle $w(\circ)$ per frame, A is the amplitude of the respective signals, $w(t)$, $r(t)$ are the received and reference monocycle waveforms with unit energy and $\tau_{m,s}$ is used to denote propagation delay from transceiver (m) to transceiver (s). A brief treatment on characterizing the propagation delay is done in [8]. We ignore pulse distortion due to differences in oscillator drift rate.

III. MEASURING ToA

The delay/Time-of-Arrival (ToA) of the transmitted monocycle at the receiver is defined relative to the beginning of the frame time. The first task involved in estimating the ToA is to coarsely measure the arrival of the monocycle at the receiver. It is followed by closed loop tracking to reduce timing jitter and improve accuracy of the timing estimation. The tracking of UWB monocycles was examined in detail in [5]. Reference [5] also pointed out that the output of the correlative timing detector is a function of the input signal amplitude and proposed a modified slope reversal amplitude estimator from [9] to first estimate and stabilize the amplitude of the received UWB monocycles.

In order to derive the coarse timing and amplitude estimators, the maximum likelihood (ML) estimator for the ToA and amplitude of the received UWB monocycle of (2a) is considered next. Using a filter with impulse response matched to $w(t)$, the log likelihood ratio is given by

$$\ln \Lambda(A, \tilde{\tau}) = (2A/N_o) \int_{-T_D}^{T_D} y(t) w(t-\tilde{\tau}) dt - (A^2/N_o) \qquad (3)$$

where $\tilde{\tau}$ is the receiver timing offset from the transmitter and the range of integration T_D is assumed to be much longer than the impulse width. Following derivations in [11], the ML estimators are:

$$\hat{\tau} = \arg \max_{\tilde{\tau}} \int_{-T_D}^{T_D} y(t) w(t-\tilde{\tau}) dt \,, \qquad (4a)$$

$$\hat{A} = \max_{\tilde{\tau}} \int_{-T_D}^{T_D} y(t) w(t-\tilde{\tau}) dt \qquad (4b)$$

This suggested the implementation shown in Fig. 1. Therefore the Cramer-Rao bound on the ToA/delay and amplitude estimates are:

$$\mathrm{var}\{\hat{\tau} - \tau\} \geq N_o \big/ (2A^2 \overline{\omega^2}) \qquad (5a)$$

$$\mathrm{var}\{\hat{A} - A\} \geq N_o / 2 \qquad (5b)$$

where $\overline{\omega^2} = \int_{-\infty}^{\infty} \omega^2 |W(\omega)|^2 d\omega / 2\pi$ is the effective squared bandwidth with unit $1/\sec^2$ and $W(\omega)$ is the Fourier transform of the UWB monocycle. The proposed measurement system, motivated by (4), is shown in Fig. 2. It consists of a slope reversal estimator/detector [9] embedded in a feedforward AGC loop. This is concatenated with a Timing-Lock-Loop (TLL) [5].

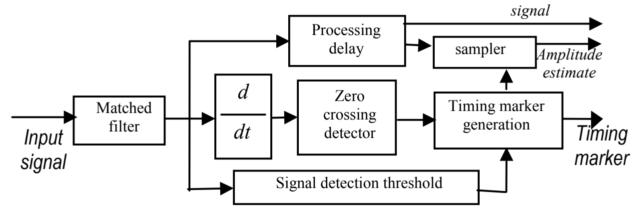

Figure 1: A modified "linear filter (slope-reversal) estimator" to estimate the time delay and amplitude of received UWB monocycle.

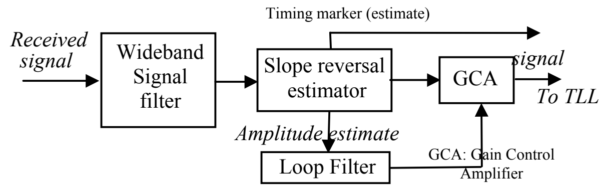

Figure 2: The Automatic Gain Control loop with the slope reversal estimator. (Feedforward Implemenation)

Substituting (2a) into (4) assuming there is no inter-frame interference, and considering the k^{th} frame, the output of the matched filter detector is:

$$g(\tilde{\tau}) = A_w A_r \int_{-T_D + t_k^{(s)}}^{T_D + t_k^{(s)}} w(t - a_1^{(m)} k' T_f - d^{(m)} - \tau_{m,s}) w(t - a_1^{(s)} k T_f - d^{(s)} - \tilde{\tau}) dt + n_k \qquad (6)$$

where A_r is the amplitude of the reference monocycle at the receiver and:

$$n_k = A_r \int_{-T_D + t_k^{(s)}}^{T_D + t_k^{(s)}} n(t) w(t - a_1^{(s)} k T_f - d^{(s)} - \tilde{\tau}) dt \,. \qquad (7)$$

For the purpose of this discussion and without loss of generality, it is assumed that $k = k'$. For this assumption to be valid, the initial offset and frame frequency differences must be within bounds that were derived in [8]. From (6) and (4a), the estimated ToA of the UWB monocycle transmitted by transmitter (m) in its k^{th} frame and received at receiver (s), and measured with respect to the start of the k^{th} frame of the receiver is given by:

$$\hat{\tau}_k = \arg \max_{\tilde{\tau}} g(\tilde{\tau}) = (a_1^{(m)} - a_1^{(s)}) k T_f + d^{(m)} - d^{(s)} + \tau_{m,s} + \xi_k \quad (8)$$

where ξ_k is the measurement error incorporating the random effect of n_k on $\hat{\tau}_k$. Note that the operation "arg max" is a nonlinear operator and $\xi_k \neq n_k$. The amplitude estimate is obtained by substituting $\hat{\tau}_k$ into (4b):

$$\hat{A}_k(\hat{\tau}_k) = \max_{\tilde{\tau}} g(\tilde{\tau}) = g(\hat{\tau}_k) \qquad (9)$$

IV. AUTOMATED GAIN CONTROL

A feedforward AGC is chosen for its stability with minimum time lag between its input and output. For the purpose of analysis, the AGC of Fig. 2 is represented in Fig. 3

using its equivalent model where $v_d(t_k^{(s)})=\hat{A}_k(\hat{\tau}_k)$ is the output of the amplitude detector evaluated at $t_k^{(s)}$ in receiver (s). Following derivation given in [1], the amplitude suppression factor of the detector is defined as the ratio of the estimated amplitude to the input signal amplitude and denoted as β_k. Then, assuming amplitude of received monocycle remains stable during measurement:

$$\begin{aligned}\beta_k &= \mathrm{E}\{\hat{A}_k \mid \xi_k\}/A_w \\ &= \mathrm{E}\{g(\hat{\tau}_k)\mid\xi_k\}/A_w = \Psi(\xi_k)\end{aligned} \tag{10}$$

where
$$\Psi(\xi_k)=\int_{-T_D+t_k^{(s)}-t_k^{(m)}-\tau_{m,s}}^{T_D+t_k^{(s)}-t_k^{(m)}-\tau_{m,s}} w(t)w(t-\xi_k)dt \tag{11}$$

which is the auto-correlation function of the UWB monocycle pulse $w(t)$. This allows us to express $v_d(t_k^{(s)})$ as:

$$v_d(t_k^{(s)})=A_w\cdot\beta_k+n_k \tag{12}$$

Note that β_k is a function of Signal-to-Noise-Ratio (SNR, defined as $A^2/(N_o/2)$) via the delay estimation error ξ and in addition a function of $w(t)$ as seen from (11) and (12).

To understand the effect of UWB monocycle pulse shape on performance, the n^{th} order Gaussian derivative UWB monocycle model, denoted as $w_n(t)$, is adopted. It has being shown in [5] that $w_n(t)$ fits the received waveform for dipole antenna well. The monocycle waveform $w_n(t)$ also offers the flexibility to adjust the pulse width of the impulse readily. The effective squared bandwidth of $w_n(t)$ is given by $\overline{\omega^2}=(2n+1)p$ [5], where $p=1/(2\sigma_w^2)$ and σ_w approximates the width of the impulse.

The function $\mathsf{M}(A_d,v_d)$, with the desired output signal amplitude denoted as A_d, is used to map the output of the amplitude detector to the input of the Gain Control Amplifier (GCA). The GCA with output denoted as $\mathsf{G}(v_c(t))$, where $v_c(t)$ is the gain control voltage, can be of various forms [1]. Here the hyperbolic gain is used:

$$\mathsf{G}(v_c(t))=\mathsf{g}_o/v_c(t) \tag{13}$$

Let the gain of the amplitude detector be G_D and without loss of generality, let $G_D=1$, then:

$$v_c(t_k^{(s)})=\mathsf{M}(A_d,v_d)=\mathsf{g}_o v_d(t_k^{(s)})/A_d \tag{14}$$

The amplitude of the signal at the output of the feedforward AGC can now be written as:

$$A_{o(k)}=\mathsf{G}(v_c(t_k^{(s)}))\cdot A_w=\frac{A_d A_w}{\beta_k A_w+n_k}=\frac{A_d A_w}{v_d(t_k^{(s)})} \tag{15}$$

If $n_k\to 0$, from (6) and (8), $\xi_k\to 0 \Rightarrow \beta_k\to 1$ and $A_o=A_d$. Some form of averaging can be implemented at the output of the AGC to average out fluctuations in $A_{o(k)}$.

The linear slope reversal estimator depicted in Fig. 1 is simulated and the results plotted in Fig. 4 for SNR from 10 to 30 dB. The search range is -2000 to 2000 sample points centered at the actual ToA position. The error in estimating the signal amplitude is negligible for most practical purposes for SNR above 20dB.

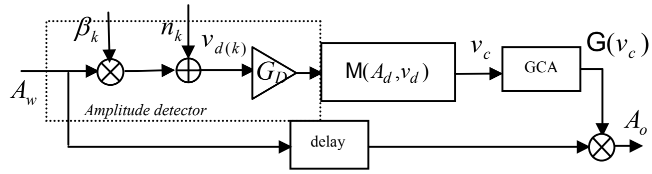

Figure 3: Equivalent representation of the Automated Gain Control loop.

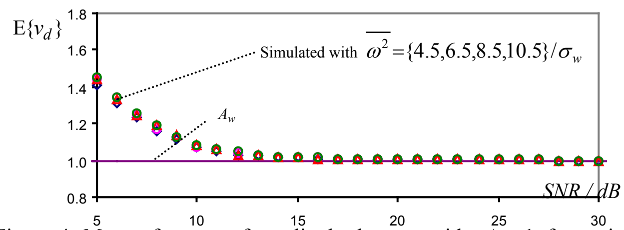

Figure 4. Mean of output of amplitude detector with $A_w=1$ for various squared bandwidth. Difference in amplitude estimate is not distinguishable for the different squared bandwidths (4.5 to 10.5)/σ_w simulated.

V. TLL Tracking With AGC

The estimated delay $\hat{\tau}_k$ from the matched filter and the received UWB monocycle after going through the AGC are feed into the timing detector. The ToA is estimated using a correlative timing detector with characteristic function (S-curve) given by:

$$s(\varepsilon)=(A_{o(k)}A_r)\int_{-\infty}^{\infty} w(t)r(t+\varepsilon)dt \tag{16}$$

where $r(t)$ is the reference signal generated at receiver. The estimate $\hat{\tau}_k$ is used to 'set' the TLL so that it operates at the linear region of the characteristic function of the correlative timing detector, i.e., during tracking the timing error ε fluctuates about the stable equilibrium point at $\varepsilon=0$ and $s(\varepsilon)$ is approximated by $s(\varepsilon)=\varepsilon\cdot s_o^{/}$ where $s_o^{/}=(ds(\varepsilon)/d\varepsilon)|_{\varepsilon=0}$. The linearized representation of the tracking loop is shown in Fig. 5. The received signal is now being tracked by the TLL and ξ in (8) is replaced by ε.

As shown in Fig. 5, the output of the correlative timing detector is:

$$x_k=K_D\cdot s(\varepsilon_k)+K_D\cdot n_k^{/}. \tag{17}$$

Without loss of generality, K_D is chosen to make the slope of the detector characteristic to be 1. However in the absence of perfect knowledge of the received signal amplitude, the receiver assumes that it is A_d, i.e., the desired signal amplitude. Therefore, detector gain is set at $K_D=1/(\mu A_d)$ where $\mu=(d/d\varepsilon)\cdot\int_{-\infty}^{\infty}w(t)r(t+\varepsilon)dt\Big|_{\varepsilon=0}$ and

$$s(\varepsilon_k)=\int_{-T_D+t_k^{(s)}}^{T_D+t_k^{(s)}} A_{o(k)}A_r w(t)r(t+\varepsilon_k)dt=A_r A_{o(k)}\cdot\mu\cdot\varepsilon_k \tag{18a}$$

$$K_D \cdot n_k^{/} = (A_d A_r / v_d(t_k^{(s)})) n_k^{//} / (A_d \mu) \tag{18b}$$

$$\varepsilon_k = (a_1^{(m)} - a_1^{(s)}) k T_f + (d^{(m)} - d^{(s)}) + \tau_{m,s} - \hat{\tau}_k^{/} \tag{18c}$$

where $n_k^{//} = \int_{-\infty}^{\infty} n(t) r(t - t_k^{(s)} - \hat{\tau}_k^{/}) dt$ and $\hat{\tau}_k^{/}$ is the adjustment make by the receiver such that $\mathrm{E}\{\varepsilon_k\} = 0$ in steady state. Note that $s(\varepsilon)$ is a function of the input signal amplitude unless $v_{d(k)} = A_w$, i.e., $A_{o(k)} = A_d$. The coefficient in front of $n_k^{//}$ arises from multiplying the received signal $y(t)$ by $A_d / v_d(t_k^{(s)})$ as a result of passing the signal through the AGC. We have made use of the tracking/linearity assumption in (18a). Let $\int_{-\infty}^{\infty} r^2(t) dt = 1$ and $A_r = 1$ in the subsequent analysis. Readers are cautioned that the correct approach to obtain the timing jitter of the ToA due to additive noise is to use superposition as in [12] because of the feedback in the system. If $Z\{u_k\}$ is the Z-transform of u_k, from Fig. 5, the loop transfer function is defined as:

$$\frac{Z\{\hat{\tau}_k'\}}{Z\{t_k^{(m)}\}} = H(\mathrm{z}) = \frac{\mu A_{o(k)} K_D D(\mathrm{z})}{1/I(\mathrm{z}) + \mu A_{o(k)} K_D D(\mathrm{z})} \tag{19}$$

It was shown in [5] that $\mathrm{E}\{\varepsilon_k^2\}$ due to additive noise is minimized when $r(t) = -dw(t)/dt$ such that

$$(\mu)^2 = \left[d/d\varepsilon \int_{-\infty}^{\infty} w(t) r(t+\varepsilon) dt \bigg|_{\varepsilon=0} \right]^2 = \overline{\omega^2} \tag{20}$$

The (opened loop, $\hat{\tau}_k^{/} = 0$) output of the timing detector x_k will then achieve the Cramer-Rao lower bound:

$$\sigma_{CR(n)}^2 = 1 \big/ (\Theta_{m,s} \overline{\omega^2}) \tag{21}$$

where $\Theta_{m,s} = 2A_w^2 / N_o$ is defined as the SNR at receiver and A_w^2 (A_o^2 if AGC is deployed) is the received signal energy. This bound is optimistic because matched filter UWB receivers are hard to build. Note that the loop noise bandwidth depends on the ratio $A_{o(k)}/A_d$ via $H(\omega)$. In Fig. 6, an example of the benefits of preceding the TLL with AGC is illustrated. It is assumed that the amplitude estimate is obtained from the $(k-1)^{\text{th}}$ frame while the TLL is tracking the k^{th} frame, thus n_{k-1} of (7) and $n_k^{//}$ of (18) are taken to be independent. The digital loop filter is of the form $D(\mathrm{z}) = G_1 + G_2 \mathrm{z}/(\mathrm{z}-1)$. Without the AGC, the performance of the TLL is degraded significantly.

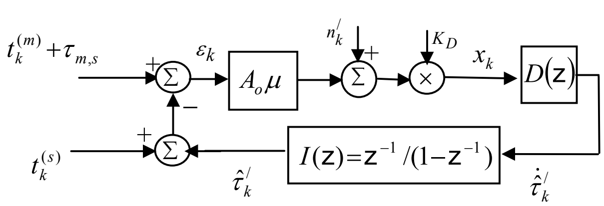

Figure 5: Equivalent timing model for the tracking of UWB impulses.

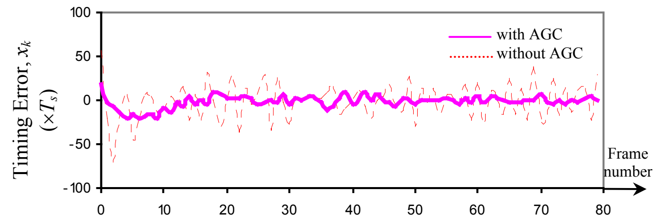

Figure 6: Output of detector x_k with and without AGC preceding second order TLL at 20 dB SNR. The gains of the filter are G_1=0.3297 and G_2=0.0736, $A_w = 3.3$, $A_d = 1$, σ_W=100T_s, n=8, $(a_1^{(m)} - a_1^{(s)}) T_f = 10 T_s$, $\zeta = 20 T_s$ where T_s is the sampling period.

VI. Frame Frequency Estimation

We assume transceivers are stationary during measurements. Then estimation of the difference in oscillator drifts can be accomplished by at least two different approaches.

One possible approach is to employ a second order TLL as described earlier and in references [1] [5] at the receiver to track the UWB pulses from the transmitter. That is, we have a 2^{nd} order TLL loop to handle mismatch between the transmitter and receiver oscillator drift (frame-repetition-rate). The transmitter will send out a sufficiently long sequence of monocycles to be pulled-in and tracked by the TLL at the receiver, which will then estimate $(a_1^{(m)} - a_1^{(s)}) T_f$ and the initial offset as follows.

To evaluate the performance of this approach, let $\gamma = (a_1^{(m)} - a_1^{(s)}) T_f$ and $\zeta = \tau + d^{(m)} - d^{(s)}$. To extract γ and ζ from the TLL, from Fig. 5, and at steady state $\mathrm{E}\{\varepsilon_k\} = 0$, then:

$$\hat{\gamma}_{TL} = \hat{\tau}_k^{/} - \hat{\tau}_{k-1}^{/} \tag{22a}$$

And
$$\hat{\zeta}_{TL} = x_o = A_o \zeta / A_d + n_k^{//} / (A_w \mu) \tag{22b}$$

In (22b), it is assumed that SNR is sufficient such that $v_d(t_k^{(s)}) \approx A_w$. To evaluate $\sigma_{\hat{\gamma}_{TL}}^2$, consider the transfer function:

$$\frac{Z\{\hat{\gamma}_{TL}\}}{Z\{n_k^{/}/(A_o\mu)\}} = \frac{\mu A_o K_D D(\mathrm{z})}{1 + \mu A_{o(k)} K_D D(\mathrm{z}) I(\mathrm{z})} = \frac{H(\mathrm{z})}{I(\mathrm{z})} \tag{23}$$

Then the variances of the estimates are:

$$\sigma_{\hat{\gamma}_{TL}}^2 = \mathrm{E}\{|\gamma - \hat{\gamma}_{TL}|^2\} \geq \int_{-\pi}^{\pi} |H(\omega)/I(\omega)|^2 \frac{N_o/2}{2\pi A_w^2 \overline{\omega^2}} d\omega \tag{24a}$$

$$\sigma_{\hat{\zeta}_{TL}}^2 = \mathrm{E}\{|\zeta - \hat{\zeta}_{TL}|^2\} = \mathrm{E}\{x_o^2\} \geq (N_o/2)/(A_w^2 \overline{\omega^2}) \tag{24b}$$

Simulation result is compared with theoretical bound of (24a) and agrees well.

The second approach can be viewed as a modification of the techniques described in [2]. A Least Squares (LS) fitting is performed on the measurements taken at the output of the correlative timing detector (The timing detector is not embedded in a TLL.), i.e., $\hat{\tau}_k^{/} = 0$ in Fig. 5 such that:

$$x_k = \gamma \cdot k + \zeta + \mathrm{v}_k \tag{25}$$

where $\gamma = \frac{A_{o(k)}}{A_d}(a_1^{(m)} - a_1^{(s)}) T_f$, $\zeta = \frac{A_{o(k)}}{A_d}(d^{(m)} - d^{(s)} + \tau_{m,s})$ and

$\mathsf{v}_k = n_k^{//} / A_w \mu$. The receiver takes successively ToA measurements x_k of the synchronization pulses from the transmitter. Following [4], a Least Squares (LS) estimator can be formulated. A recursive implementation of the LS estimator can be found in [4]. However, the simplicity of the LS estimator in this application leads to simple batch processing without computing any matrix inverses. It can be shown that the LS estimates are:

$$\hat{\gamma}_{LS} = 12\sum_{k=1}^{K} k \cdot x_k / (K(K^2-1)) - 6\sum_{k=1}^{K} x_k / (K(K-1)) \tag{26a}$$

$$\hat{\varsigma}_{LS} = 2(2K+1)\sum_{k=1}^{K} x_k / (K(K-1)) - 6\sum_{k=1}^{K} k \cdot x_k / (K(K-1)) \tag{26b}$$

The estimation error variance, if variance of v_k is bounded using (21), is given by:

$$\sigma^2_{\hat{\gamma}_{LS}} = \mathrm{E}\{(\gamma - \hat{\gamma}_{LS})^2\} \geq (12/(\Theta_{m,s}\overline{\omega^2}))\Big/(K(K^2-1)) \tag{27a}$$

$$\sigma^2_{\hat{\zeta}_{LS}} = \mathrm{E}\{(\zeta - \hat{\zeta}_{LS})^2\} \geq (2(2K+1)/(\Theta_{m,s}\overline{\omega^2}))\Big/(K(K-1)) \tag{27b}$$

Note that $\hat{\gamma}_{LS}$ and $\hat{\zeta}_{LS}$ are scaled by A_o / A_d. The Cramer-Rao bound of (21) is the lower bound on the timing jitter of the opened loop correlative timing detector, while the LS estimator is estimating parameters γ and ζ given the ToAs' estimate. According to [4], if the mapping from parameter to measurement space is deterministic and v_k has zero mean and is independent identically distributed, then the LS estimator is unbiased and an efficient estimator within the class of linear estimators. Thus equations (27a) and (27b) are indeed tight lower bounds. Reference [10] has derived a Cramer-Rao bound on estimating the difference in oscillator drift between a pair of transceivers by digitally sampling the received monocycles and minimizing the least squares. It has the same expression as (27a) when the sampling rate is allowed to go to infinity to generate the continuous time bound. Here the bound on the initial offset is obtained as well.

In Fig. 7, the theoretical bounds at different K as given by (27) are plotted alongside an averaged (over 3000 realizations) simulation computed using (26) for $\sigma_{\mathsf{v}} = \sqrt{\mathrm{E}\{\mathsf{v}^2\}} = 1.176T_s$, $\Theta_{m,s} = 30\ dB$, $\overline{\omega^2} = 8.5/\sigma_w^2$, $\sigma_w = 100T_s$, $(a_1^{(m)} - a_1^{(s)})T_f = 10T_s$, $\tau_{m,s} + d^{(m)} - d^{(s)} = 20T_s$ where T_s is the sampling interval. The corresponding normalized standard deviation on $\hat{\gamma}$ obtained using TLL with parameters specified in Fig. 6 (unless indicated otherwise) is also indicated in Fig. 7. The variance using TLL is much higher than the LS approach although it can be reduced by reducing the loop bandwidth. It should be noted that both approaches are not able to separate the propagation delay τ from $d^{(m)} - d^{(s)}$ in ζ. Other techniques as described in [8] are needed to obtain the initial offset between transceivers' local oscillators.

In the LS approach to estimate γ and ζ, the output of the estimator is scaled by A_o/A_d. To ensure convergence of the TLL, the AGC is needed to stabilize the loop gain as illustrated in Fig 6.

The TLL is able to control the convergence of the tracking error while a fixed number of frames are needed to reach the required error variance in the LS approach. The LS technique on the other hand approaches the Cramer-Rao bound and analysis of the error variances of the TLL preceded with AGC is made difficult due to the non-linearity involved in estimating the delay using a matched filter.

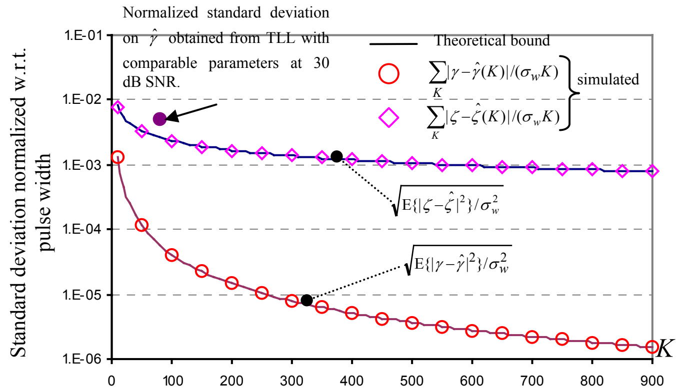

Figure 7: Normalized standard deviation of Least Squares estimator for γ and ζ. The standard deviation of the measurement error is $\sigma_{\mathrm{v}}=1.176T_s$ secs at SNR of 30 dB where T_s is the sampling interval, K is the number of frames and $\hat{\gamma}(K)$ and $\hat{\zeta}(K)$ are used to denote the estimated parameters using the LS estimator for K frames.

ACKNOWLEDGEMENT

This work benefited from comments from Bob Weaver.

REFERENCES

[1] Heinrich Meyr and Gerd Ascheid, *Synchronization in Digital Communications – Volume 1, Phase-, Frequency-Locked Loops, and Amplitude Control*, Wiley 1990.

[2] F. Mazzenga, F. Vatalaro and C. E. Wheatley, III, "Performance Evaluation of a Network Synchronization Technique for CDMA Cellular Communications", *IEEE Trans. Wireless Commun.*, vol. 1, No. 2, April 2002.

[3] Zhi Tian, Liuqing Yang & G.B.Giannakis, "Symbol Timing Estimation in Ultra Wideband Communications", *Proc. Asilomar Conf. Signals, Systems, and Computers,* 2002.

[4] J. M. Mendel, *Lessons in Estimation Theory for Signal Processing, Communications, and Control*, Prentice Hall, 1995.

[5] Chee-Cheon Chui and Robert A. Scholtz, "Optimizing Tracking Loops for UWB Monocycles", *Proc. IEEE Globecom*-2003.

[6] Chee-Cheon Chui and Robert A. Scholtz, "Tracking UWB Monocycles in IEEE 802.15 Multi-path channels", *Proc. Asilomar Conf. Signals, Systems, and Computers,* 2003.

[7] Joon-Yong Lee and R. A. Scholtz, "Ranging in a Dense Multipath Environment using an UWB Radio Link", *IEEE J. Select. Areas Commun.*, vol. 20, No. 9, Dec 2002.

[8] Chee-Cheon Chui and R. A. Scholtz, "A Synchronizing Scheme for an Impulse Network", *Proc. MILCOM*, 2004.

[9] Eli Brookner (Editor), *Radar Technology*, Artech House, Chapters 6 and 11, 1978.

[10] Antonio A. D'Amico and Umberto Mengali, "Frame Frequency Estimation in Ultra-Wideband Systems", 2004 (unpublished).

[11] H. L. Van Trees, *Detection, Estimation and Modulation Theory, Part 1*, Wiley.

[12] Robert M. Gagliardi, *Satellite Communications*, 2nd Edition, USC Custom Publishing.

[13] W. C. Lindsey and C. M. Chie, "Theory of Oscillator Instability Based Upon Structure Functions", *IEEE Proc.*, Dec 1976.